SYNCHROTRON-RADIATION PHOTON DISTRIBUTION FOR HIGHEST ENERGY CIRCULAR COLLIDERS*

G. H. I. Maury Cuna#, CINVESTAV, Merida, Mexico
D. Sagan, G. Dugan, CLASSE, Cornell University, Ithaca, NY, USA
F. Zimmermann, CERN, Geneva, Switzerland

Abstract

At high energies, beam-induced synchrotron radiation is an important source of heating, beam-related vacuum pressure increase, and primary photoelectrons, which can give rise to an electron cloud. The photon distribution along the beam pipe wall is a key input to codes such as ECLOUD and PyECLOUD, which model the electron cloud build-up. For future high-energy colliders, like TLEP or SHE-LHC, photon stops and antechambers are considered in order to facilitate cooling and vacuum pressure control. We use the Synrad3D code developed at Cornell to simulate the photon distribution for the LHC.

INTRODUCTION

The code Synrad3D newly developed at Cornell University has been employed to track synchrotron radiation photons generated at storage rings and linacs [1, 2]. The code permits estimating the energy deposition and position distribution of photon absorption sites, which are key inputs to simulate the electron cloud build-up. Synrad3D includes photon scattering from the vacuum chamber surface, based on X-ray data from LBNL [3] for computing the reflectivity of a smooth surface and an analytical model [4, 5] for diffuse scattering from a surface with finite roughness. Synrad3D can handle non-planar lattices and a wide spectrum of vacuum chamber cross sections. Thanks to its versatility, the code can also be used to predict the radiation environment for a proton beam in the LHC arcs.

In the following sections, we describe the general approach and models used for computing both the specular and the diffuse reflection, and we present a first application of the program for calculating the radiation environment of the LHC arc.

SCATTERING MODEL

Synrad3D uses Monte Carlo techniques to generate (macro-particle) photons based on the standard synchrotron radiation theory for relativistic charged particles traversing regions of different magnetic fields, in the lattice of an accelerator. Photons are generated with respect to the closed orbit of the particle beam. The particle beam size and divergence are taken into account when generating the photon starting positions and momenta, respectively.

Similar to the program PHOTON [6], photons are tracked until they hit the vacuum chamber walls. There, in Synrad3D the probability of being scattered and the scattering angle, are determined by the incident photon's energy and angle of incidence, computed from the models described below, while in PHOTON only specular reflection at a constant (input) probability had been considered.

Photon Reflectivity

The probability of a photon being reflected from a wall is dependent upon the grazing angle and the photon energy. For a given graze angle and photon energy, there are two reflection probabilities called $P_{reflect}$ and $R_{specularr}$, both determining the probabilities that a photon will be reflected, either specularly ($P_{reflect} \cdot R_{specular}$) or diffusely [$P_{reflect} \cdot (1 - R_{specular})$], or that the photon will be absorbed ($1 - P_{reflect}$).

In general, the value of $P_{reflect}$ is near unity at small grazing angles on a smooth surface and falls off with increasing angle. At smaller photon energies ($E \lesssim 100$ eV), i.e. for most photons in the LHC, with a critical photon energy of 44 eV (at 7 TeV proton-beam design energy), the reflection probabilities will still be substantial at grazing angles of 10 degrees or more. At larger photon energies ($E \gtrsim 1000$ eV), the reflection probabilities are quite peaked and small above a few degrees. The probability of specular reflection of a photon from a rough surface depends on the rms surface roughness σ, the photon wavelength λ, and the grazing angle. It is modelled by equations

$$R_{specular} = \mathrm{e}^{-g(x)}, \quad (1)$$

$$g(x) = \frac{16\pi^2\sigma^2x^2}{\lambda^2}. \quad (2)$$

In which x is the cosine of the incident polar angle, and the angle of reflection equals the angle of incidence. The diffuse scattering model used in Synrad3D is based on scalar Kirchhoff theory. In the code we assume Gaussian distributions for both the surface height variations (rms σ) and the transverse distribution (taken to be equal in both transverse directions, with autocorrelation coefficient T). In Figs. 1 and 2, we show example scattering-probability curves for different photon energies as a function of the grazing angle. This curves correspond to a 10 nm C layer on Cu substrate (σ=200 nm).

*Work supported by CONACYT, EPLANET and EuCARD projects.
#gmauryc@mda.cinvestav.mx

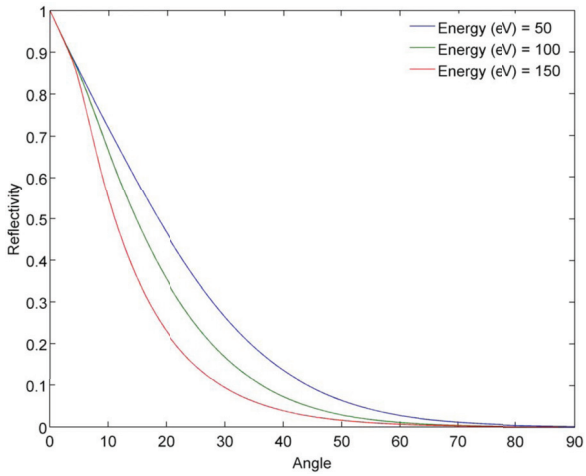

Figure 1: Total reflection probability ($P_{reflect}$) vs. grazing angle at three different photon energies for a 10 nm layer of C on Cu substrate, values taken from [3]

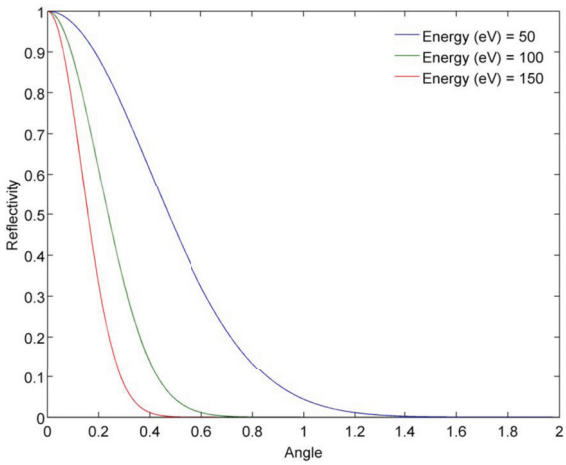

Figure 2: Specular reflection probability ($R_{specular}$) vs. grazing angle at three different photon energies from equations (1) and (2).

METHODOLOGY

Synrad3d was used to obtain the photon absorption points. The version 6.5 of the LHC optics was employed. The cross section of the LHC arc beam screen is depicted in Fig. 3 All the simulations were performed for 7 TeV proton beam energy. The parameter values for $P_{reflect}$ were taken from the LBNL X-ray database [3] assuming a C layer of 10 nm on a Cu substrate [7,8], which is expected to form during electron-cloud "scrubbing" [9]. An rms surface roughness of 200 μm was considered. The special LHC "sawtooth pattern" [10,11], a series of 30-μm high steps spaced at a distance of 500 μm in the longitudinal direction, which is impressed on the horizontal outer side of the beam-screen, at the primary impact point of the radiation, was not included here.

RESULTS FOR LHC ARCS

Figure 4 displays the distribution of total photon absorption sites; the distribution is uniform and a 17% of photons are absorbed at the bottom and top edges. Figure 5 shows a histogram of the number of reflections. We can observe that though a large number of photons is absorbed at the first encounter with the beam pipe, many other photons are reflected several times before being absorbed. The mean number of reflections is about 60. In Fig. 6, we present a histogram of the energy of the absorbed photons, with a long tail of several tens of eV, which should correspond to the emission spectrum. In Fig. 7, we show the distribution of the photon absorption sites along an LHC arc of length 2.45 km for the dipole sections. We got similar distributions for quadrupole and drift sections. A build up saturating near the centre of the arc is predicted. The differences between a dipole, quadrupole and a drift section along an LHC, primarily reflect the respective fraction of the arc covered by these fields (dipole: ~81%, quadrupole: ~8%, drift: ~11%). In table 1, we list the percentage of total absorption sites per magnetic environment, we can see those values are similar to the fraction of the arc covered for each section.

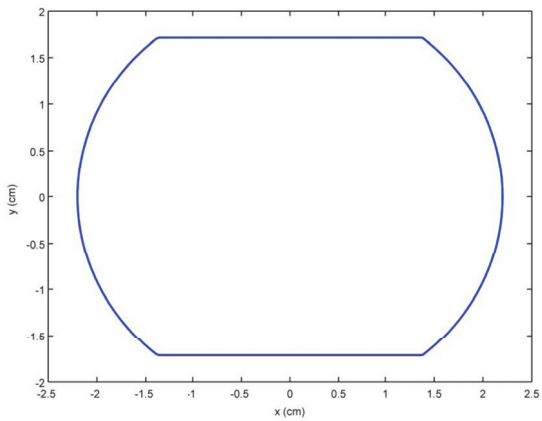

Figure 3: Shape of the LHC beam screen in the cold arcs

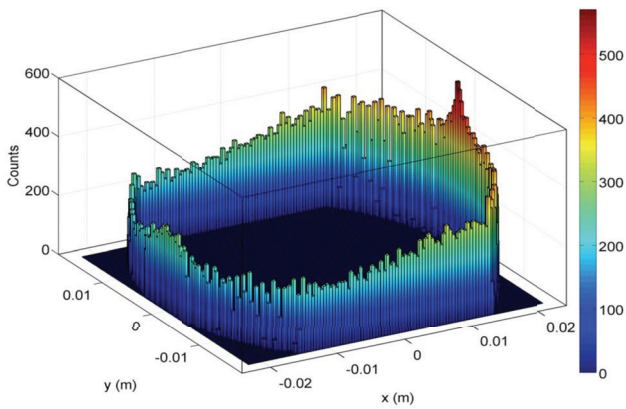

Figure 4: Distribution of total photon absorption sites.

Table 1: Comparison Per Magnetic Environment

Section	Fraction of total absorbed photons (%)	Arc fraction covered (%)
Dipole	81.7	81
Drift	10.5	11
Quadrupole, etc.	7.8	8

ISBN 978-3-95450-122-9

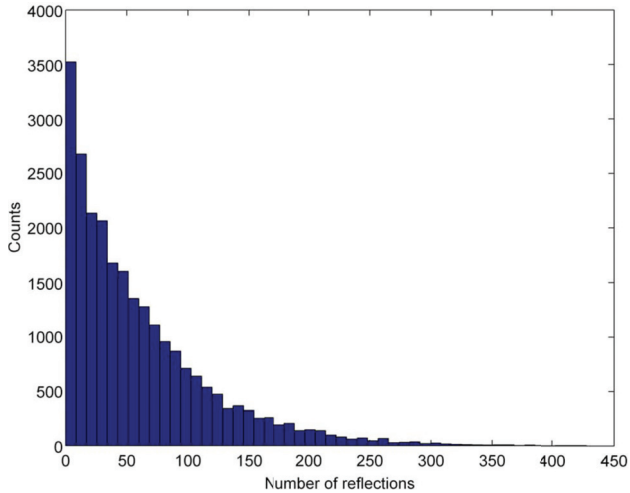

Figure 5: Histogram showing the number of photon reflections before absorption.

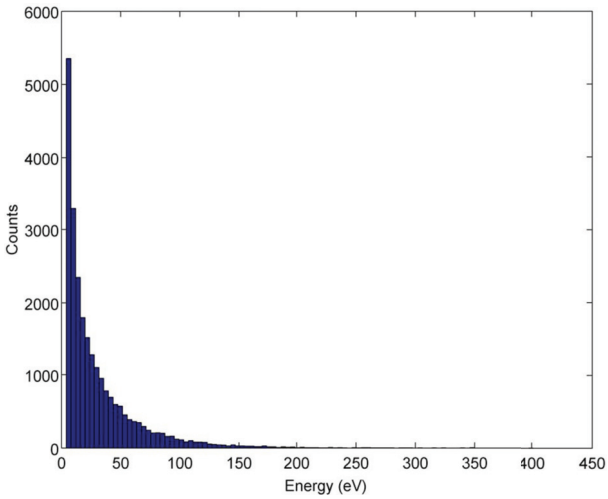

Figure 6: Energy distribution of the absorbed photons.

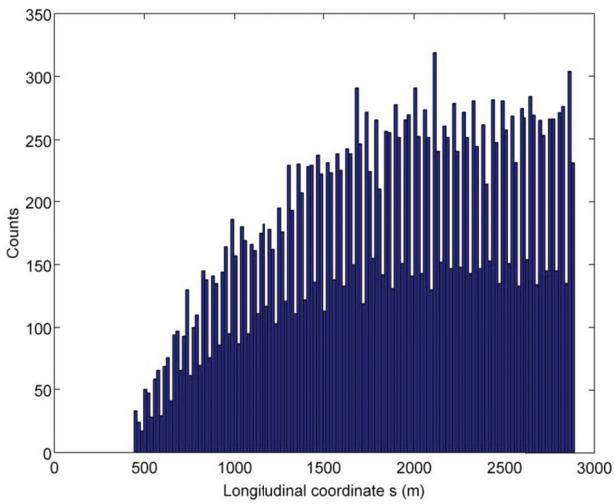

Figure 7: Distribution of photon absorption sites for dipole sections.

FUTURE WORK

We have employed the code Synrad3D for a first photon distribution analysis of the LHC arcs. The current version of the code can model different LHC beam-pipe cross sections. Also, as an option, the special sawtooth pattern has been implemented. In the coming months the simulation work with Synrad3D for LHC will be extended and, in particular, simulations for the full ring will be performed. In addition, we plan to investigate the photon distribution for higher-energy circular colliders, like VHE-LHC (100 TeV *pp* collider in an 80/100-km tunnel) and TLEP (an e^+e^- collider with up to 350 GeV c.m. energy installed in the same tunnel).

ACKNOWLEDGMENTS

This work has been supported in parts by the Mexican Council of Science and Technology CONACYT, by the European Commission under the FP7 Research Infrastructures project EuCARD, grant agreement no. 227579, and by the European Particle Physics Latin American NETwork EPLANET and CINVESTAV. Synrad3D development supported by the US National Science Foundation (PHY-0734867, PHY-1002467, and PHY-1068662), and US Department of Energy. One of us (G.H.I.M.C.) would like to extend special thanks to Elizabeth Castañeda Miranda, Sergio Rioja Fuentelsaz and Silvano Roubatel for their great support and friendship.

REFERENCES

[1] G. Dugan and D.Sagan,"SYNRAD3D Photon Tracking Program", Tech. rep., Cornell University (2012), http://www. lepp.cornell.edu/~dcs16/synrad3d.pdf
[2] G. Dugan et al., "Observations and Predictions at CesrTA, and Outlook for ILC," in Proceedings of ECLOUD'12, La Biodola, Elba, Italy (2012).
[3] http://henke.lbl.gov/optical_constants/layer2.html
[4] P. Beckmann & A. Spizzichino, The Scattering of Electromagnetic Waves from Rough Surfaces, Pergamon Press, New York (1963).
[5] J. A. Ogilvy, Theory of Wave Scattering from Random Rough Surfaces, Hilger, Bristol (1993).
[6] F. Zimmermann, Synchrotron radiation in the LHC Arcs - Monte Carlo Approach, LHC-Project-Note-237 (2003).
[7] R. Cimino, private communication (2013).
[8] R. Larciprete *et al.*, Secondary electron yield of Cu technical surfaces: Dependence on electron irradiation, Phys. Rev. ST Accel. Beams 16, 011002 (2013).
[9] G. Iadarola e*t al.*, Electron Cloud and Scrubbing Studies for the LHC, IPAC'13 Shanghai, these proceedings.
[10] V. Baglin, I. Collins, O. Gröbner, Photoelectron Yield and Photon Reflectivity from Candidate LHC Vacuum Chamber Materials with Implications to the Vacuum Chamber Design, Proc. EPAC98, Stockholm (1998) p. 2169
[11] O.S. Brüning *et al.*, LHC Design Report, v.1: The LHC Main Ring, CERN-2004-003-V-1 (2004), Chapter 5.